Hydrogels as a water bolus during hyperthermia treatment

Physics in Medicine & Biology

PAPER • **OPEN ACCESS**

Hydrogels as a water bolus during hyperthermia treatment

To cite this article: Hana Dobšíek Trefná and Anna Ström 2019 *Phys. Med. Biol.* **64** 115025

IOP Publishing Phys. Med. Biol. 64 (2019) 115025 (14pp) https://doi.org/10.1088/1361-6560/ab0c29

Physics in Medicine & Biology

IPEM Institute of Physics and Engineering in Medicine

OPEN ACCESS

PAPER

Hydrogels as a water bolus during hyperthermia treatment

Hana Dobšíček Trefná[1] and Anna Ström[2,3]

[1] Department of Electrical Engineering, Chalmers University of Technology, Göteborg, Sweden
[2] Department of Chemistry and Chemical Engineering, Chalmers University of Technology, Göteborg, Sweden
[3] SuMo BIOMATERIALS, VINN Excellence Center, Chalmers University of Technology, Göteborg, Sweden

E-mail: hanatre@chalmers.se and anna.strom@chalmers.se

Keywords: microwaves, mechanical properties, dielectrical properties

RECEIVED
6 October 2018

REVISED
22 February 2019

ACCEPTED FOR PUBLICATION
4 March 2019

PUBLISHED
31 May 2019

Abstract

The feasibility of using hydrogels as a water bolus during hyperthermia treatment was assessed. Three types of gels, high methoxyl (HM) pectin/alginate, xanthan/locust bean gum (LBG) and xanthan/LBG/agarose were evaluated based on their dielectric, rheological and mechanical properties. The most suitable, xanthan/LBG/agarose gel was further used as a water bolus in a hyperthermia array applicator. The gels composed of polysaccharides carrying low charge displayed dielectric properties close to those of water, while the dielectric properties of HM pectin/alginate gel was deemed unsuitable for the current application. The mechanical examination shows that the xanthan/LBG gel has a non-brittle behaviour at room temperature, in contrast to the agarose gel. The moduli of the xanthan/LBG gel weaken however considerably between the temperature range of 40 °C and 50 °C, reducing its potential to be used as water bolus. The ternary system of xanthan/LBG/agarose had advantageous behaviour as it was dominated by the thermal hysteresis typical of agarose upon temperature increase, but governed by the typical non-brittle behaviour of the xanthan/LBG at low temperatures. The final evaluation within the hyperthermia applicator showed excellent signal transmission from the antennas. The agarose/xanthan/LBG gel reduced the scattering of electromagnetic waves, enabled a tight closure between the body and the antennas, and offered a less bulky solution than the currently used water-filled plastic bags. The results presented here open up a new application area for hydrogels in improving heat delivery during hyperthermia treatment and other near-field microwave applications.

1. Introduction

Hyperthermia, i.e. elevation of the tumor temperature to 40 °C–44 °C has been shown to be among the most effective radiosensitizers known today (Overgaard 2013) as well as an enhancer of many cytotoxic drugs (Kampinga 2006). The beneficial effect of adding hyperthermia to radiotherapy or chemotherapy has been demonstrated in a number of clinical studies for a large variety of tumors (Cihoric *et al* 2015, Datta *et al* 2016). Hyperthermia inhibits repair of DNA damage caused by radiotherapy and induces changes in perfusion and re-oxygenation, thereby enhancing radiosensitivity (Dewhirst *et al* 2005). Furthermore, it leads to increased blood flow and vessel permeability, which in turn improve the delivery of the chemotherapy drug to the tumor (Kampinga 2006).

To achieve temperature elevation, electromagnetic (EM) or ultrasound energy is emitted to the target tissue. The EM heating utilizing frequencies in the range of 1–1000 MHz, i.e. radiofrequency (RF) and microwave (MW) bands, is the most frequently applied technique, clinically available for treatment of most tumor sites. For superficial heating associated with tumor depths of approximately 2–4 cm, single antennas or array applicators placed on the surface of the body are typically employed. Deeper penetration in the body is then achieved by using constructive wave interference from a large number of antennas organized in multiple rings around the patient, so called phased array applicator.

As the antennas are placed in the close proximity of the patient, heating of the body surface is, due to conductive and dielectric losses, inevitable and therefore the body surface needs to be cooled. In addition, a matching

medium between the applicator and the body is required to couple the EM energy to the tissue. In hyperthermia, the above is solved by the circulation of a deionised/demineralized water through plastic or silicone bags placed between the antenna applicator and the body, a so called water bolus. Despite recent improvements in water bolus designs (Arunachalam *et al* 2009, Rijnen *et al* 2015), several drawbacks are associated with this set-up: (a) bulky and irreproducible bolus shape, which hamper tight contact between tissue and bolus or bolus and applicator thus giving rise to air pockets disturbing the EM field propagation and (b) disturbance of the EM fields from the plastic material.

Hereby, we report results showing that the use of hydrogels as water bolus, is a potential solution for above mentioned drawbacks with current water boli. Hydrogels contain a high amount of water, and their viscoelastic character enables a close fit to the skin. While hydrogels has been used as tissue-mimicking phantom material when studying the effect of EM fields on biological tissues (Hellerbach *et al* 2013), the performance of hydrogels as water bolus has, as far as the authors are aware, never been examined.

A range of polysaccharides, many of which are non-toxic and readily available, form hydrogels. In this study, we focused on gels prepared from alginate/pectin, xanthan/locust bean gum (LBG), and agarose. These polysaccharides are extensively used in the food, pharmaceutical, and biomedical sectors (Draget and Taylor 2011, Lee and Mooney 2012, Hermansson *et al* 2016).

The alginate/pectin is a synergistic gel formed upon acidification of pH below *pKa* of the polysaccharides, approximately pH 3.5 (Morris and Chilvers 1984, Walkenström *et al* 2003, Ström *et al* 2009). The synergistic gels are favoured in the presence of highly methoxylated (HM) pectins (Ström and Williams 2004) and with alginate containing a high amount of guluronate (Walkenström *et al* 2003). Xanthan gum forms synergistic and thermoreversible gels in the presence of galactomannans, such as LBG (Copetti *et al* 1997, Wielinga 2009). The strength of the xanthan/LBG gels varies depending on the xanthan to LBG ratio (Lundin and Hermansson 1995, Copetti *et al* 1997), whether the polysaccharides are mixed hot or at room temperature (Mannion *et al* 1992, Zhan *et al* 1993), as well as the content of pyruvate and acetate of the xanthan (Fitzpatrick *et al* 2013, Renou *et al* 2013) and the galactose content of the LBG (Goycoolea *et al* 1995, Lundin and Hermansson 1995). The exact nature of the interaction between the xanthan and LBG has been debated (Cairns *et al* 1986, Goycoolea *et al* 1995, Renou *et al* 2013) but it involves a direct molecular interaction (Cheetham *et al* 1986, Goycoolea *et al* 1995, Higiro *et al* 2006), meaning that it is not related to incompatibility of the two polysaccharides. Agarose forms strong gels under cooling, and its gelation is related to the formation of fibers originating from helices of agarose. The gels exhibit thermal hysteresis, i.e. they melt at a higher temperature compared to their gelation temperature (Watase and Nishinari 1983, Norton *et al* 1986), a feature to be exploited in the present application. The hysteresis in setting and melting of the agarose gel has been attributed to aggregation of agarose helices (Watase and Nishinari 1983, Norton *et al* 1986, Normand *et al* 2003).

While the overall characteristics of above mentioned gels are well described, little is known about their dielectric properties, which are crucial for their utilization in RF and MW systems. In addition, the impact of temperature elevation on the rheological properties of the gels during treatment need a careful examination as well as the behaviour of the gels when exposed to a constant stress (both stress and heat generated from the antennas). Here, we report the dielectric properties of the above mentioned gels, the rheological properties as a function of temperature, as well as their stress relaxation behaviour. A solution for enhanced heat transfer was proposed and verified in a realistic experiment with a hyperthermia applicator including antennas and a muscle tissue-mimicking phantom. To the best of our knowledge, this is the first work showing the use of hydrogels as water bolus during hyperthermia treatment.

2. Materials and methods

2.1. Materials

Alginate is composed of (1–4)-linked β-D-mannuronic acid and α-L-guluronic acid derived from seaweed (Draget 2009). The alginate used in this study was Manugel DMB, which has a high guluronate content and was provided by FMC BioPolymer, Norway.

Commercially available pectin is mainly composed of homogalacturonan (1–4)-linked α-D-galacturonate). Pectin is further divided into low-methoxyl or high-methoxyl (HM) pectin depending on the methylation degree of the galacturonate (Ström and Williams 2004). The HM-pectin used in this study was a research sample obtained from CP Kelco, Denmark and was derived from citrus fruit. It had a methylester content of 76% according to the supplier.

Xanthan gum is composed of a (1–4)-linked β-D-glucose backbone with a trisaccharide chain on every other glucose at C-3, containing a glucuronic acid residue linked (1–4) to a terminal mannose unit and (1–2) to a second mannose that connects to the backbone (Sworn 2009). Xanthan gum is an extracellular polysaccharide secreted by the bacterium *Xanthomonas campestris*. LBG is composed of a linear (1–4)-linked mannose backbone with a single D-galactopyranosyl unit attached via-(1–6) linkages as a side branch (Wielinga 2009).

Table 1. Composition (in % w/vol) of tested gels, where HM pectin = high methoxyl pectin and LBG = locust bean gum.

Gel	Alginate	HM pectin	Xanthan	LBG	Agarose
HM pectin/alginate	1.32	0.68	—	—	—
Xanthan/LBG	—	—	0.5	0.5	—
Xanthan/LBG/Agarose 1	—	—	0.40	0.40	0.20
Xanthan/LBG/Agarose 2	—	—	0.39	0.39	0.22
Xanthan/LBG/Agarose 3	—	—	0.38	0.38	0.24
Agarose	—	—	—	—	1

Both the xanthan gum (GRINDSTEDT MAS-SH A35300) and the LBG (GRINDSTED 246) were provided by DuPont, Denmark. The xanthan sample had a pyruvate content of 5% according to the supplier.

Extracted from red seaweed, agarose is composed of repetitive units of D-galactose and 3,6 anhydro-L-galactose, and was purchased from Sigma-Aldrich, Sweden, as was D-glucono-δ-lactone (GDL).

2.2. Gel preparation

All polymers were slowly added to deionized water at room temperature under vigorous stirring. The dispersions were heated to 95 °C and kept at this temperature until the polymers were fully dispersed (typically 30 min). Thereafter, they were they kept at 4 °C until further use.

Three types of gel were prepared; HM-pectin/alginate, xanthan/LBG and xanthan/LBG/agarose. The HM-pectin/alginate gels were prepared at a final polymer concentration of 2% in a polymer ratio of 2:3 (alginate:HM-pectin). GDL was added to the alginate/HM-pectin dispersion at a concentration to obtain a final pH of between 3.5, as previously described (Ström *et al* 2009). This solution was subsequently mixed and immediately used for (a) tests using small deformation rheology (in this case, the gel was let to set on the rheometer) or (b) poured into moulds of 10 mm in diameter and 10 mm in height for stress–strain measurement or (c) poured into moulds of 34.5 mm in diameter and height of 13 mm for testing of its dielectrical properties.

Xanthan/LBG gels were obtained by mixing xanthan and LBG dispersions at a 1:1 ratio, ending at a total polymer concentration of 1%. The lower polysaccharide concentration chosen for the xanthan/LBG system compared to the HM-pectin/alginate is related to the high viscosity of xanthan resulting in difficulties of mixing and dissolving the polysaccharides. Indeed, xanthan forms weak gel properties already at concentrations above 0.3% (Goycoolea *et al* 1995). The ratio of 1:1 of xanthan:LBG was chosen as this specific ratio has shown to favour high gel strength (Mannion *et al* 1992, Copetti *et al* 1997). Similarly as to the HM-pectin/alginate gels, the xanthan and LBG dispersions were heated to 95 °C and mixed at 90 °C for 15 min under stirring before being poured into moulds and cooled. Mixing the polysaccharides hot has shown to be favourable for gel strength compared to mixing them at room temperature (Mannion *et al* 1992). Xanthan/LBG and agarose gels were prepared similarly as above, but the agarose was always added to the already mixed xanthan/LBG dispersion at 90 °C. While the final polymer concentration was fixed at 1%, xanthan/LBG and agarose gels were prepared with different polymer ratios (as presented in table 1).

2.3. Gel properties

Dielectric properties: To model interaction between biological tissue and EM fields, a macroscopic model involving the dielectric properties, i.e. relative permittivity ϵ_r and conductivity σ is often used. The permittivity describes the polarization effects on charged particles owing to the applied field, and the conductivity describes the electrical losses in the material owing to the currents driven by the field. The dielectric properties of the gels were determined by an open-ended coaxial dielectric probe (85070E, Dielectric Probe Kit with Performance Probe, Agilent Technologies, USA) connected to a vector network analyzer (VNA) (E8362B, Agilent Technologies, USA). The properties were measured at 101 points in the frequency range of 300 MHz to 2 GHz. Each examined gel was firmly attached to the probe, to avoid air pockets on the boundary between the probe and the gel.

Rheology: The rheological properties were determined by comparison of the storage (G′) and loss (G″) moduli of the gels at given temperature range. The rheometer used was Physica MCR 300 with a cone and plate geometry (Anton Paar, Germany). The cone had a diameter of 50 mm and an angle of 1°. The measurement was done at a gap of 50 μm, a frequency of 1 Hz, and a strain of 0.5%. The hot (90 °C) xanthan/LBG and xanthan/LBG/agarose dispersions were loaded at 60 °C to a pre-heated plate and cone (60 °C). The gelation was followed as the temperature was reduced to 15 °C with 5 °C min^{-1} and kept for 10 min after which the system was reheated again to 60 °C with 5 °C min^{-1}. In contrast, the HM-pectin/alginate systems were loaded at 20 °C as this gel sets upon reduction in pH and not temperature. The reduction in pH was achieved via the use of GDL and the gel was left to set over night.

Mechanical testing: Uniaxial stress relaxation was performed on all gels using a texture analyser (TA-HDi, Stable Micro Systems, UK) and with a load cell of 5 kg. Stress–strain curves were obtained using uniaxial compression with an Instron mechanical test frame (model 5565A). Both tests were done in three repeats. Gels were formed by pouring hot polymer solution into cylindrical moulds of 10 mm in height and 10 mm in diameter and let to set for 24 h at room temperature. The gels were carefully removed from the moulds before testing and aligned in the center of stainless steel compression plates. The plates were lubricated with mineral oil to allow free expansion of the gels when compressed. Stress relaxation of the samples were studied at compression of 20, 30 and 40% strain using an initial crosshead speed of 4% strain/second. The stress response upon relaxation of the gel was studied for up to 300 s. The stress (σ_s) was calculated from the force curve by $\sigma_s = \frac{F}{A_0}$ with F being the force used to compress and maintain the sample compressed at each strain studied and A_0, the initial area of the sample. The modulus (G) was calculated from $G = \frac{\sigma}{\gamma}$ where γ corresponds to the strain. G_{max} is defined at the highest value of G upon compression and G_{relax} at $t = 300$ s. Stress relaxation was performed on three different gels for each polysaccharide composition. The stress–strain curves were obtained at a cross-head speed of 4% strain/second. True stress was calculated using $\sigma_{true} = \frac{FH}{A_0 H_0}$ and true strain was calculated from $\gamma = ln\frac{H}{H_0}$ with H and H_0 being samples height and initial height respectively.

Heat transfer: An important function of a water bolus is to cool the body surface from heat caused by dielectric losses. Due to the relatively low thermal conductivity of water-based materials (ca 0.5 W (m K)$^{-1}$), the cooling ability of the gel itself is insufficient. In order to control/manage the skin temperature, we introduced a water circulation through prefabricated channels inside the gel. The ability of the xanthan/LBG/agarose gel to effectively transfer heat was evaluated with gel dimensions of 230 × 80 × 30 mm. Two channels of diameters 8 mm were placed symmetrically along the gel at a distance of 12 mm from the center. The channels were achieved by the insertion of plastic rods inside the molds prior to casting of the gel, the plastic rods were carefully removed once the gel was set. In order to test the cooling capability of the gel, the gel was placed on the lower back of a healthy volunteer, as visualized in figure 5(a). The initial gel temperature was around 23 °C, while the body surface body temperature was 36 °C). Six fiberoptic probes with a diameter of 0.8 mm (FISO Technologies, Canada) were inserted inside the gel to measure the temperature evolution during the experiment. Two of the probes were placed along the central axis (T5, T6) while the remaining four sensors were situated at the sides, at approximately in the half of the distance between the channels and the edge of the gel. The temperature distribution of the gel surface was further accessed by infrared (IR) camera (FLIR, B335, FLIR Systems, USA). The gel was perfused with water at a temperature of 11 °C flowing through both channels with a flow rate of 0.4 m s^{-1} for 10 min.

2.4. The hyperthermia array applicator with hydrogel as water bolus

The feasibility of the xanthan/LBG/agarose gel to fulfill the function of water bolus during hyperthermia treatment was investigated in two cases: in a single antenna setup figure 6(b) representing the superficial hyperthermia and within a phased array applicator figure 6(d) devoted to deep heating.

The first experiment follows the standardized setup for applicator testing (Trefna *et al* 2017a, 2017b). A water bolus with dimensions 300 × 100 × 20 mm was placed on the top of muscle phantom with dimensions 300 × 300 × 100 mm. The relative permittivity of the phantom ϵ_r was 59.1 at frequency 550 MHz, while the electrical conductivity σ of 0.75 S m^{-1}. A single self-grounded Bow-Tie antenna operating at frequency band of 450–850 MHz was placed on the top of the water bolus (Takook *et al* 2017), as illustrated in figures 6(a) and (b). The experiment was carried out at room temperature, with the phantom being at equilibrium with room temperature at the start of the experiment. Water ($T = 25$ °C) was circulated through the enclosure of the antenna to prevent its overheating, but no water cooling was applied to the gel, in order to imitate the worst case scenario. The antenna was operated at frequency of 550 MHz with input power of 75 W for 15 min, with the reflected power variation between 5 to 10 W.

Finally, the gel with dimensions of 360 × 180 × 50 mm placed was arranged in the phased array applicator (Trefna *et al* 2016), to verify that it can serve as a water bolus even in the more challenging arrangement. The setup, visualized in figures 6(c) and (d), included a bolus between the antennas and the cylindrical muscle phantom with a radius of 50 mm and length of 300 mm. The relative permittivity of the phantom ϵ_r was 59.2 at 500 MHz, while the electrical conductivity σ was 0.72 S m^{-1}. The hyperthermia applicator consisted of 10 independently controlled self-grounded Bow-Tie antennas that operates in frequency band of 450–850 MHz (Trefna *et al* 2016). The antennas were arranged in two circular rings with distance of 30 mm, in order to focus energy in the target region. The amplitudes and phases were controlled by the prototype of a wideband multi-channel amplifier system with maximal output power of around 100 W (Trefna *et al* 2012). Prior to the heating experiment the effect of additional plastic layer was accessed by placing a thin latex layer (below 1 mm) between the hydrogel and antennas, see figure 6(d). After measurement of reflection coefficients of all antennas with the VNA (ZNBT-8, R&S, Germany), this additional layer was removed and reflection coefficients of all antennas were re-measured.

The reflection coefficient is a parameter that describes how much of an electromagnetic wave is reflected by an impedance discontinuity in the transmission medium.

The heating experiment was performed with the later setup, i.e. without the latex layer according to the standard verification procedure for heating equipment. The muscle phantom was pre-cut in the middle plane of the antenna array to allow for determination of the heat distribution in the phantom directly after the exposure. We aimed to focus the energy in the center of the muscle phantom; thus all antennas radiated the same power of 7 W with equal phases at a frequency of 500 MHz for 7 min. The cooling by the water circulation through the gel was not applied.

3. Results

3.1. Dielectric properties

Figure 1 shows the relative permittivity, ϵ_r, and electrical conductivity, σ, of the examined gels. The ϵ_r of all the examined gels is highest at a frequency of 300 MHz and decreases slightly with increased frequency. Although the xanthan/LBG/agarose gel exhibits the highest permittivity ($\epsilon_r = 83.8$), this value is relatively close to the permittivity of distilled water ($\epsilon_r = 81$). The conductivity of the xanthan/LBG gels is slightly higher than that of deionized (DI) water, namely 0.09 S m^{-1} versus 0.02 S m^{-1} at 300 MHz, and it increases with frequency as is typical for all water-based materials in the present frequency band. The addition of agarose to the mixture does not affect the conductivity of the gel. The conductivity of the HM-pectin/alginate gel is notably higher, in particular 0.25 S m^{-1} at 300 MHz.

3.2. Rheological properties

During hyperthermia, a water bolus facing the skin is typically not exposed to temperatures higher than 43 °C. However, the temperature between the bolus and the antenna might be higher. Therefore, the rheological and mechanical stability of the gels needs to be maintained at temperatures up to 60 °C. Figure 2 summarizes the rheological properties of the gels in the temperature range of 20 °C–65 °C, comparing G′ and G″ moduli of the gels.

Gelation of HM-pectin/alginate was achieved by the addition of GDL, lowering the pH of the system to below four (Ström *et al* 2009). The GDL was quickly dispersed in the HM pectin/alginate solution and the mixture was added to the rheometer at room temperature and left to set over night. Figure 2(a) shows that the HM-pectin/alginate gel is characterised as a strong gel at $T = 20$ °C, with a low tan δ (tanδ = G″/G′) thus dominated by its elastic component. Increasing the temperature to 60 °C shows a reduction in both moduli, but with remaining domination of the elastic component.

As the xanthan/LBG gels are formed upon cooling, the hot xanthan/LBG was directly loaded onto the rheometer at 65 °C, followed by a temperature decrease to 20 °C. As visible from figure 2(b), the onset of gelation occurred at temperature just below 60 °C. The G′ increases as the temperature is reduced to 15 °C and tan δ is reduced from 0.8 at 60 °C to 0.04 at $T = 15$ °C. Increasing the temperature from 20 to 60 °C results in a reduction of both moduli. Limited thermal hysteresis is observed, in agreement with previous studies (Goycoolea *et al* 1995).

From figure 2(c) it is obvious that an absolute value of G′ of the pure agarose gel with a tan δ of 0.03 is similar to that of the HM pectin/alginate gel. The gel sets at a temperature of about 40 °C, thus at a lower temperature compared to the xanthan/LBG. The onset of gelation is here taken at the temperature at which G′ increases rapidly. Thermal hysteresis is observed upon reheating of the agarose gel, in perfect agreement with previous studies (Normand *et al* 2003).Similarly to the HM-pectin/alginate gel, G′ of the agarose gel remains high upon increase in temperature. The HM/pectin and the agarose gels were however shown to be brittle, limiting their use in the present application as it was difficult to fit the gels closely to the body without fracturing the gel.

Addition of agarose to the xanthan/LBG was intended to improve the strength and add thermal hysteresis to the pure xanthan/LBG system. This effect is indeed shown in figure 2(d), in which 0.24% agarose was added to the original xanthan/LBG solution. It can be seen that G′ of this ternary system increases to some extent, while G″ remains at similar level as the pure xanthan/LBG system. In addition, the results suggest that the addition of agarose to xanthan/LBG gel creates thermal hysteresis, thus allowing for strong gel at a broader temperature interval.

In order to investigate whether the addition of agarose is of additive or synergistic behaviour, we further determined G′ of a pure agarose gel and pure xanthan/LBG gel at the concentrations used in the ternary gel of xanthan/LBG/agarose, i.e. 0.24% of agarose and 0.76% of xanthan/LBG (table 2). The results show that G′ of the ternary system is increasing only at the low temperatures and that its value is close to the sum of G′ of the single systems of agarose and xanthan/LBG. The results thus indicate that the two networks do not disturb each other nor form synergistic associations but appear additive in behaviour. Upon reheating, one can observe that the ternary system is somewhat stronger compared to the sum of the two single systems. The values are however cor-

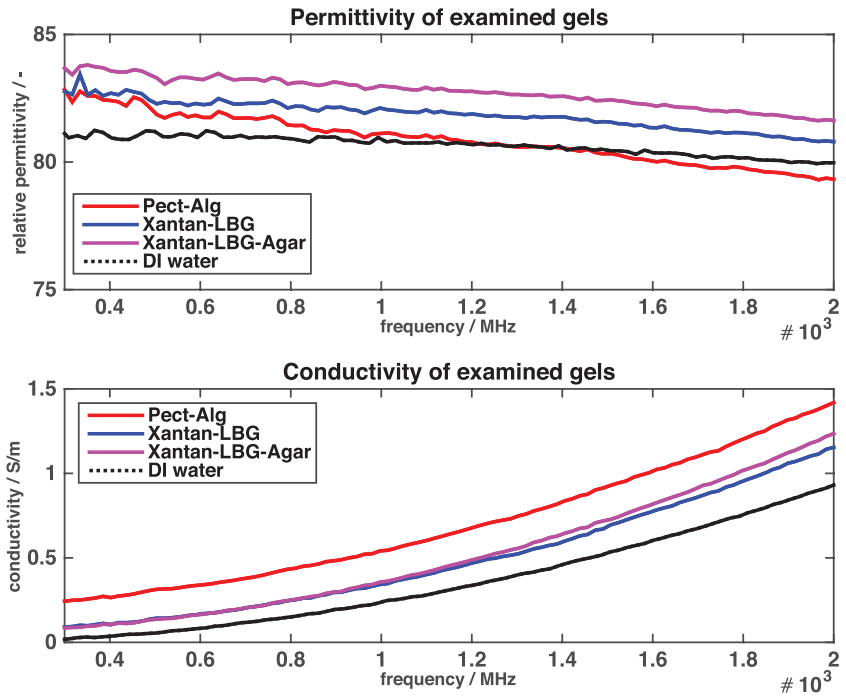

Figure 1. The dielectric properties of the examined gels.

relative if a variation between measurements of 10% is taken into account. The thermal hysteresis of the agarose gel is observed also for the single agarose gel of 0.24%, indicating that the thermal hysteresis of the ternary system is owing to the presence of agarose.

3.3. Mechanical properties

The gels need to support the weight and pressure from the antennas while still being easy to handle. Stress–strain curves and stress relaxation of the gels were therefore carried out to examine the mechanical behaviour of the gels upon compression and compression over time.

Figure 3 displays the representative stress–strain curves for agarose, xanthan/LBG and xanthan/LBG/agarose gels. The agarose gels fracture at a strain of approximately 35%. The value of strain at break is slightly higher than previously reported values of Watase and Nishinari (1983) (10% and 20%), but in agreement with values (30%–40%) reported by Normand *et al* (2003). In contrast, the gels formed from xanthan/LBG and xanthan/LBG/agarose can be compressed to a high deformation (90%) without an obvious fracture occurring in the gel, showing a non-brittle behaviour.

The stress relaxation behaviour of the agarose and xanthan/LBG gels is shown in figure 4(a). The reduction in force required to deform the gel over time can be either related to expulsion of fluid from the gel and/or reorganization of the physical network (Zhao *et al* 2010, Strange *et al* 2013). Since no expulsion of fluid was observed, the reduced force is likely to be related to network reorganization. As a result, such gel will not reform to its initial height after the force is removed.

As expected, the force required to deform the agarose gel to 20% is higher compared to the force required to deform the xanthan/LBG gel. The large difference between G_{max} and G_{relax} obtained for the agarose gels is depicted in figure 4(b). In the case of xanthan/LBG (figure 4(c)), one can observe that the difference between G_{max} and G_{relax} is relatively low and that both moduli increases with strain. The material thus appears to harden upon added strain.

The stress relaxation of the ternary systems with different mixing ratios of xanthan/LBG and agarose was tested (figure 4(d)). The total polymer concentration was kept to 1%, while the xanthan/LBG ratio was fixed at 50:50. As the agarose ratio increases, the xanthan/LBG content is reduced. The results indicated an increase in both G_{max} and G_{relax} at agarose concentrations of 0.1%–0.5% while G_{relax} was relatively high thus dominated by xanthan/LBG. Thus, the addition of agarose at intermediate concentrations leads to increased compression strength of the gel while maintaining the non-brittle behaviour typical of the pure xanthan/LBG system. Note that the results are shown in log-log scale to facilitate the comparison of the different systems.

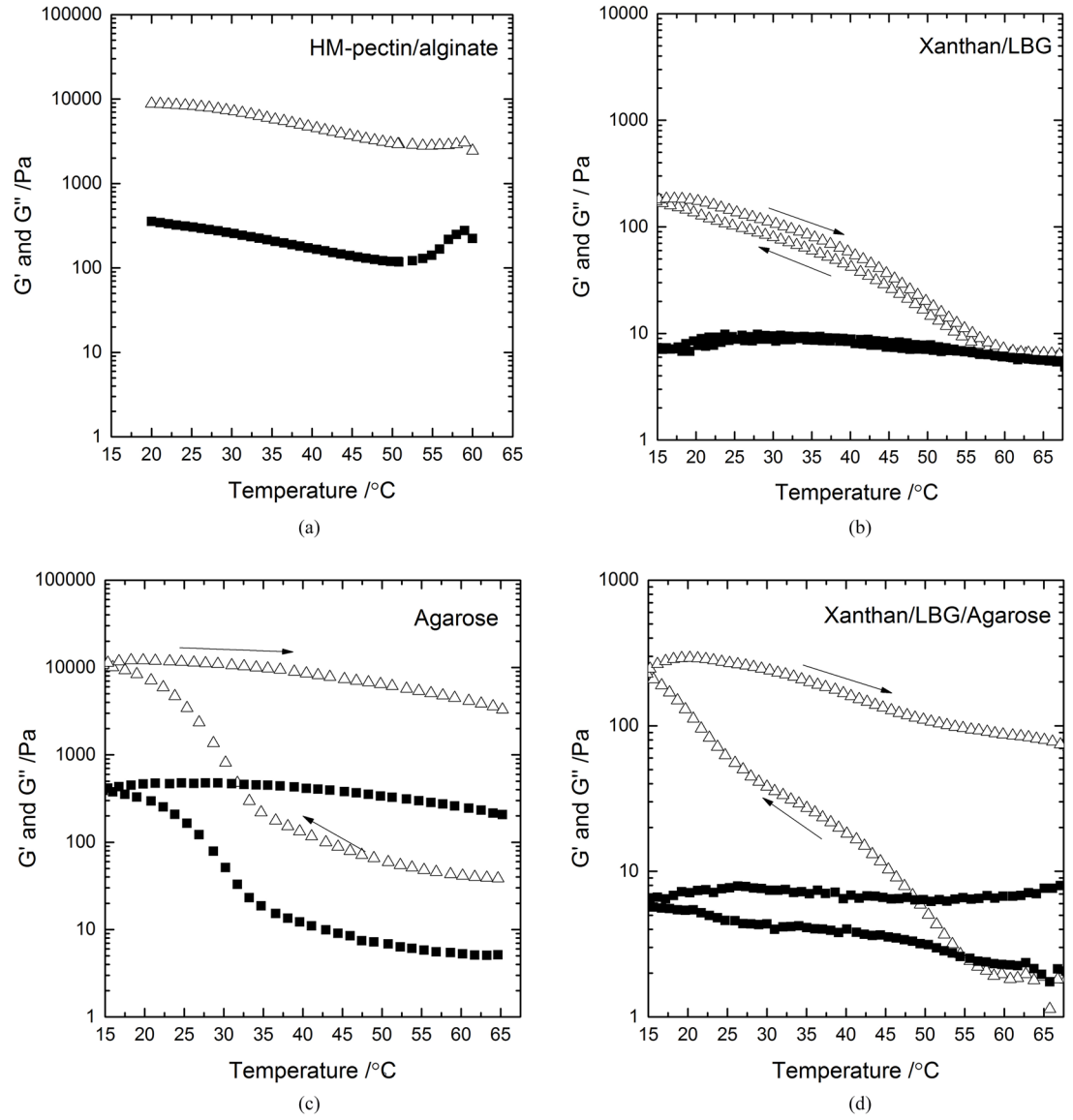

Figure 2. G′ (open triangles) and G″ (solid squares) as a function of temperature of (a) HM-pectin and alginate gel (b) xanthan/LBG gel (at a 1% total polymer conc. and a ratio of 1:1), (c) agarose (1%), (d) xanthan/LBG/agarose (at a total polymer conc of 1% and a ratio of 1.6:1.6:1). Measurements were performed at a strain of 0.5% and $f = 1$ Hz and with temperature sweeps of 5 °C min^{-1}.

Table 2. Storage moduli, G′, at different temperatures for single system of agarose (0.24%), xanthan/LBG (a ratio of 50:50 and total polymer conc. of 0.76%) and ternary system of xanthan/LBG/agarose at a total of 1% polymer concentration. Expected variations between measurements are 10%.

Temp. /°C	Agarose G′ /Pa	Xanthan/LBG G′ /Pa	Agarose/xanthan/LBG G′ /Pa
Cooling			
60	<1	2	2
50	<1	5	4
40	4	20	20
20	70	70	130
Heating			
20	180	110	350
40	160	30	210
50	140	10	160
60	120	2	145

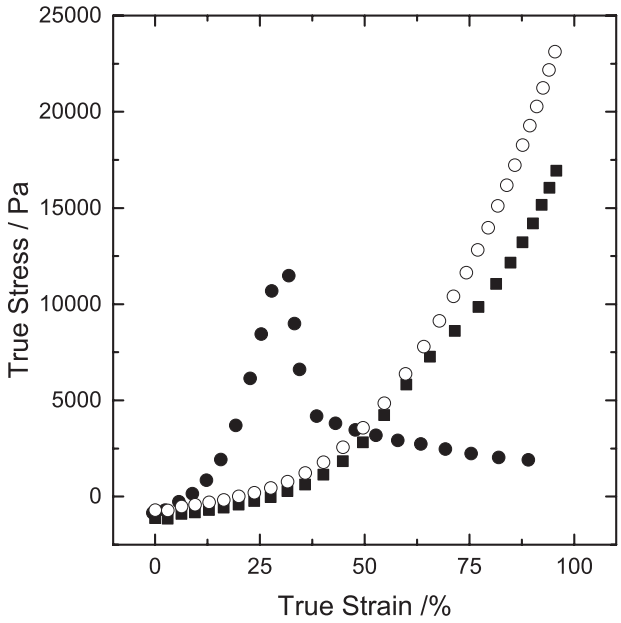

Figure 3. True stress and true strain of the agarose gel (filled circles), xanthan/LBG (filled squares) and xanthan/LBG/agarose (open circles). Total polymer concentrations at 1% .

3.4. Heat transfer

The ability of the xanthan/LBG/agarose gel to effectively cool the body surface was examined in a setup shown in figure 5(a). The temperature differences in different parts of gel during cooling were measured with fiberoptic probes (T1–T6) and further supported by thermographic images. It is worthwhile to mention that the absolute temperatures measured by the IR camera and the temperature probes are not in perfect agreement due to absolute accuracy of $\pm 2°$ of the IR camera. The results from the experiments are therefore presented in terms of relative temperature differences.

The fibre-optic probes indicated a temperature decrease of 7 °C during 10 min at the center of the phantom (T5 and T6) from the initial bolus temperature. A temperature decrease achieved alongside the bolus was lower, about 34 °C. For better understanding of the temperature profiles, the temperature distribution of the gel was recorded by IR camera in two situations: the surface temperature distribution of the gel after 10 min of cooling (figure 5(b)) and the skin temperature immediately after the gel was turned over and placed adjacent to the site on the body (figure 5(c)). In both figures, the two channels for water cooling are visible as two dark-blue sections with the lowest temperatures. As suggested in figure 5(c), the lowest skin temperature of 22 °C was achieved along the cooling channels, while the remaining part under the bolus had a temperature of a few degrees higher. In the same figure, one observes a warmer spot in the position of the spine (pointer Sp2) with a skin temperature of about 27 °C. This indicates that the water bolus did not follow the body contour appropriately at this location leading to less efficient cooling.

3.5. Hyperthermia array applicator with hydrogel as water bolus

Figure 7 summarizes results obtained with the single applicator arrangement after 15 min of heating. An appropriate function of the antenna in the setup with the gel is illustrated by the thermographic image of the vertical cross section of the muscle phantom (figure 7(a)). The image, taken directly after the exposure, suggests temperature increase of 25 °C in 15 min and expected heating profile (Takook *et al* 2017) of the antenna. The surface temperature of the bolus on the side attached to the phantom exceeded 47 °C, while the bolus temperature under the antenna was somewhat lower due to the antenna cooling as visible from figure 7(b). The antenna imprint of the gel surface is noticeable, figure 7(c), in contrast to the other side of the gel, that remained unaffected. Observe, two imprints of the antenna in the figure 7(c), due to replacement of one antenna after approximately 10 min of heating while assessing the surface temperature of the gel. The antenna imprints became less visible after a short period of time after leaving the gel at room temperature and disappeared completely after 24 h.

In the final experiment, the xanthan/LBG/agarose gel was placed within the phased array applicator surrounding the muscle phantom in two setups: with and without an additional latex layer placed between antennas and the gel as visible from figure 6.

The reflection coefficients of all antennas were recorded and the average, maximal and minimal values over the operational frequency band of antennas were plotted in figure 8(a). The setup without additional latex layer results in lower, thus better, reflection coefficients at all examined frequencies. The maximal average reflection

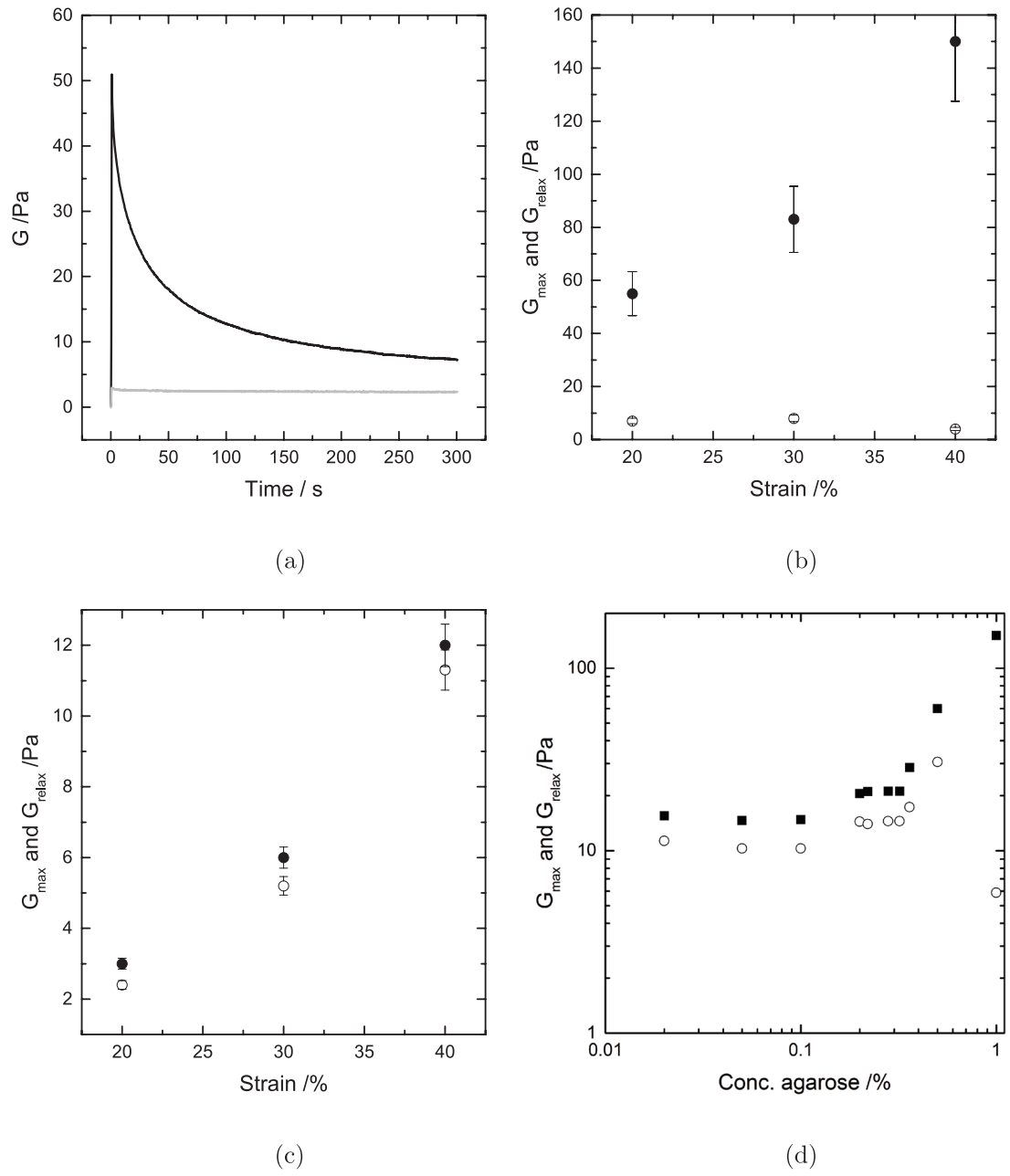

Figure 4. Stress relaxation of (a) agarose (black line) and xanthan/LBG gel (grey line) at a strain of 20% and G_{max} (filled symbol) and G_{relax} (open symbol) of (b) agarose at different strains, (c) xanthan/LBG at different strains and (d) xanthan/LBG with increasing amount of agarose at strain of 40%. The total polymer concentration was kept at 1% and the xanthan/LBG was used at ratio 50:50. All tests were done at room temperature.

for the gel-only case was −8.3 dB at 590 MHz while the worst case with additional latex layer was −7.65 dB at 583 MHz. Thus, about 16% more power was reflected back towards the antennas due to the thin plastics.

The thermal distribution in the center of the muscle phantom after exposure at 500MHz is shown in figure 8(b). The temperature increase of about 6 °C in 7 min was achieved in the focal area in the centre of the phantom. The associated temperature increase on the surface of the phantom is typical for the microwave heating without surface cooling. Observe, that the phantom edge in the picture is bounded by yellow contour. The red background is caused by highly reflective background material on which the split phantom was placed.

4. Discussion

In this study we evaluated three types of gels to serve as a water bolus during hyperthermia cancer treatment. The permittivity of all the evaluated gels was similar to the permittivity of distilled water, while the electrical conductivity of the gels was somewhat higher. The electrical conductivity of HM-pectin/alginate was an order of magnitude higher than the one of deionized water, which together with brittleness made the gel unsuitable for the present application.

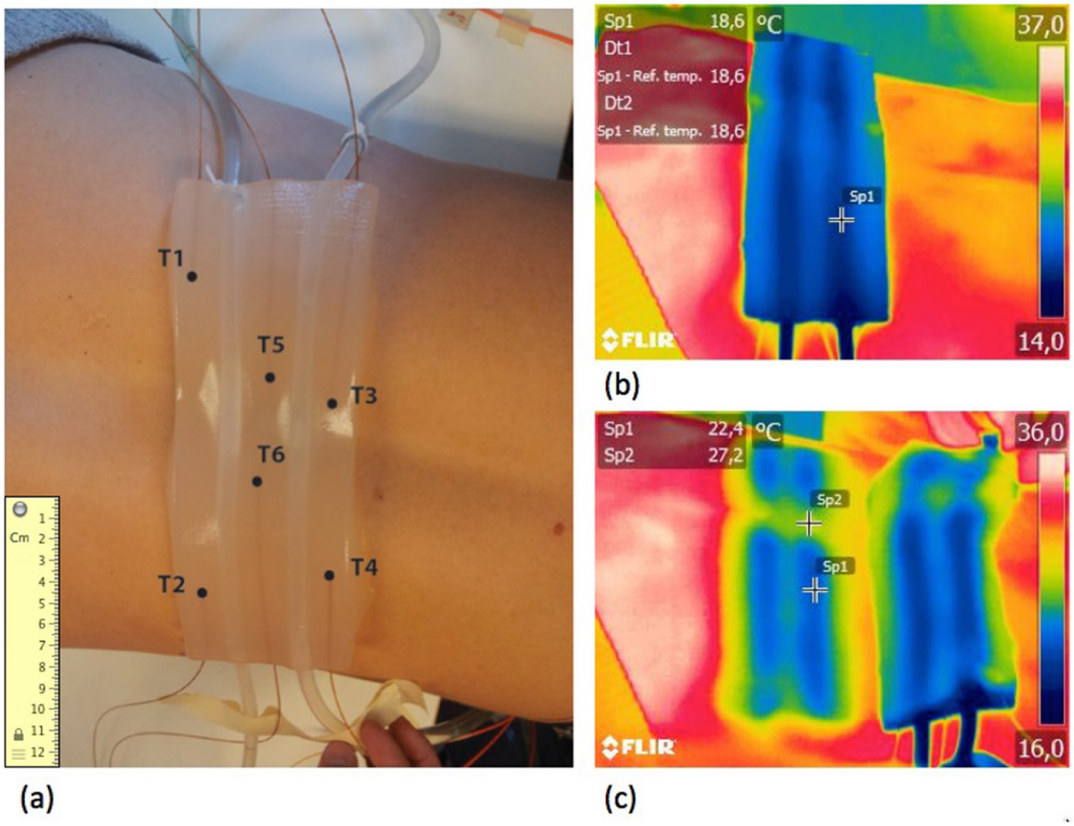

Figure 5. (a) Gel placed on the low back of a healthy volunteer with temperature probes inserted in the gel. (b) Thermographic image of the gel obtained after 10 min and (c) Thermographic image taken immediately after the gel was removed from the body.

In general, the measured electrical conductivity of the different gels are in agreement with their theoretical charge densities coupled with the absolute amount of polymers used in the present study. Alginate carries a carboxyl group on each monosaccharide unit (Draget 2009). The HM-pectin in this study carry a carboxyl group on approximately 24% of the monosugars. Hence, the HM-pectin/alginate gel have the higher amount of carboxyl groups of the gel systems used here. Xanthan, on the other hand, is only weakly charged, carrying a glucuronic acid residue on the trisaccharide side chain connected to every other glucose of the backbone and further contains pyruvate to a maximum of 50% of the terminal mannose residues (Labille *et al* 2005, Sworn 2009), and can be considered as a low-conductive. As the backbone of agarose and LBG is uncharged (Serwer 1983, Fatin-Rouge *et al* 2003), the xanthan/LBG and the xanthan/LBG/agarose gels were expected to exhibit low electrical conductivity, which was indeed demonstrated (figure 1).

While the dielectric properties of the xanthan/LBG and xanthan/LBG/agarose gels were similar, the xanthan/LBG/agarose system have the added benefit of retaining its gel strength at higher temperatures. For the hyperthermia applications, we aimed to shift the reduction in moduli to higher temperatures as typical for agarose gels, while maintaining the non brittle feature of the xanthan/LBG gels. The stress–strain curves show the large difference in fracture strain between the agarose (fracture at 35%) and the xanthan/LBG gel (no fracture observed for up to 90% strain). Mixing the xanthan/LBG with agarose shows, that if the agarose concentration is kept $<0.4\%$ the properties of the xanthan/LBG network are maintained with the added benefit of a slightly higher G of the mixed gel also at room temperature. These features facilitate handling of the gel as well as making it possible for close fitting around antennas and bodies. The addition of agarose to the gel allowed for a final, ternary system, that combines the desirable properties of the two gel types.

The xanthan/LBG/agarose gel was made in a realistic scale ($230 \times 80 \times 30$ mm), to examine whether the water cooling within the gel is achievable. Water was pumped through the channels with silicone tubes connected to the input and output of the gel, i.e. with no plastic present inside the gel. The skin temperature was reduced by 7 °C during 10 min, showing the ability of the gel to cool the body surface through heat transfer. However, the heat transfer obtained via channels through the gel may be insufficient in case of several antennas operating at maximum power levels. The diameter as well as the distance between the cooling channels remains to be optimized for a specific applicator and/or region treated, or cooling of the gel may need to be supported by other means, in our applicator design, all individual antennas were kept at low temperatures of 10 °C–15 °C through water circulation. As the antennas are firmly attached to the gel, a heat transfer is induced in large area of the gel

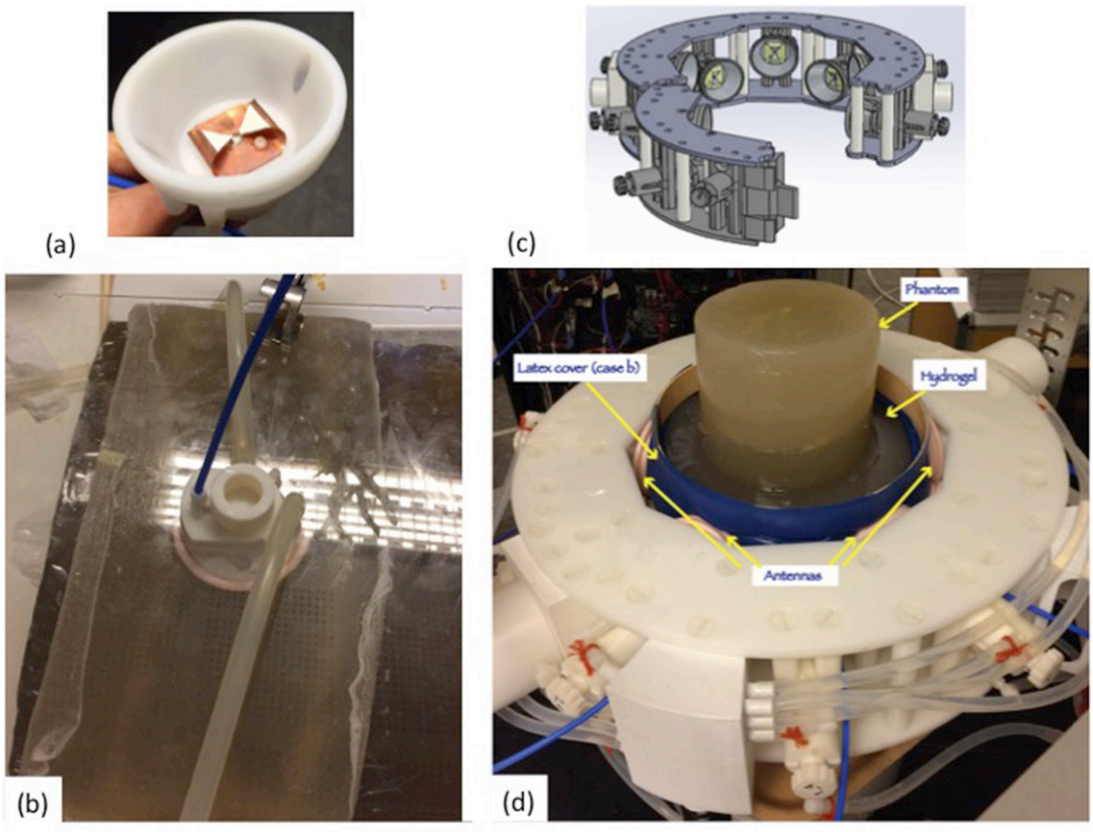

Figure 6. The xanthan/LBG/agarose gel serving as a water bolus during single applicator setup. (a) The Self grounded Bow-Tie antenna. (b) The standardized setup for applicator verification with xanthan/LBG/agarose gel placed between antenna and phantom (c) The sketch of the neck applicator prototype. with single the thermal profile of the bolus surface after 15 min of heating. (d) The xanthan/LBG/agarose gel surrounding the muscle phantom inside the hyperthermia applicator during heating experiment.

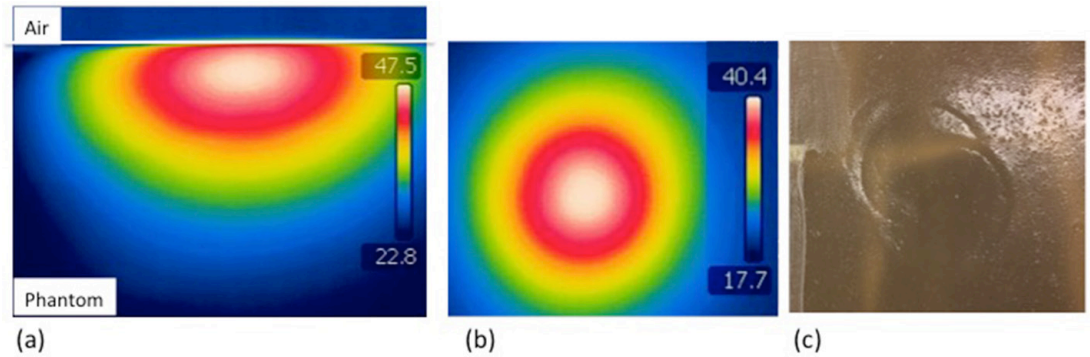

Figure 7. The xanthan/LBG/agarose gel surrounding the muscle phantom inside the hyperthermia applicator during heating experiment. (a) Thermographic image of the vertical cross-section of the muscle phantom after exposure. (b) Thermographic image of the top of the hydrogel after the exposure. (c) The photograph of the surface of the bolus after the exposure.

from the cooling of the antennas. The efficiency of this solution is observable from the heating experiment in the single antenna setup. Despite the cooling with water at around 22 °C, the temperature at the bolus surface below the antenna was about 8 °C lower than the temperature on the other side of the bolus.

An essential requirement for a proper function, matching and cooling, is an excellent contact between the gel and the body. In phased array applicators, a patient specific mould attachable to the applicator may be a solution to achieve both effective cooling and reproducible patient positioning. The latter is of great importance as an incorrect patient positioning inside the applicator can diminish the advantage of using the treatment planning tool and cause patient burns.

The temperature above 40 °C along with pressure from the antenna caused an observable imprint of the antenna in the surface of the gel, while the other side of the gel remained unaffected at significantly higher temperatures. Due to the non-plastic behaviour of the xanthan/LBG, the gel regain its original properties if left

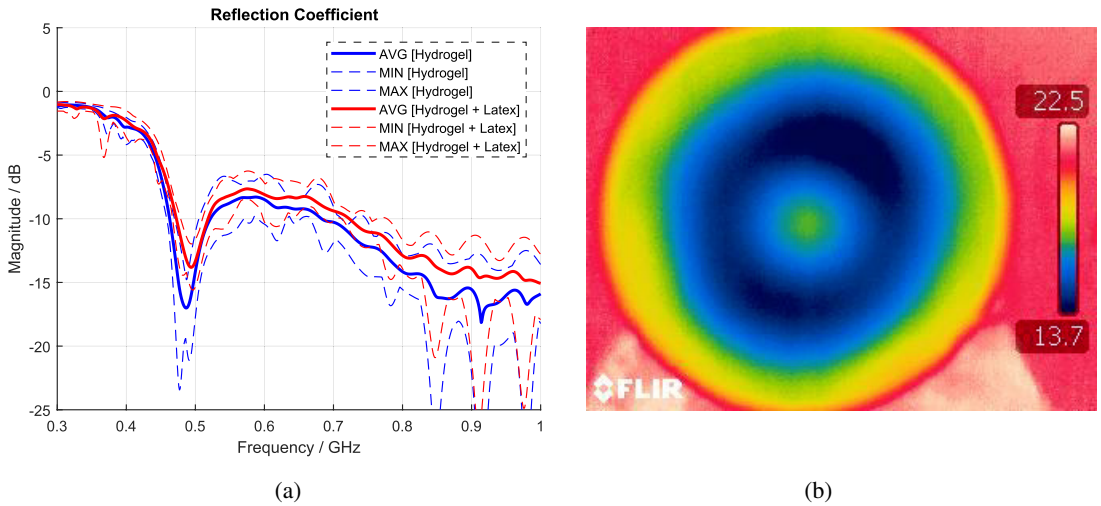

Figure 8. (a) Reflection coefficients of antennas in setup with and without latex layer. (b) Thermographic image of the cross-section of the muscle phantom exposed to heating from antenna system of 8 min. The antennas were set to focus the energy in the centre of the phantom.

at room or lower temperatures within few minutes. During the course of treatment i.e. 4–5 weeks, the gel may change its original shape, leading to a less perfect match to the body of the patient or to the antennas. In such a case, the xanthan/LBG/agarose gel can be melted at $T = 95$ °C and re-casted into the patient specific mould as it is thermally reversible. Typically, we have been using the gels with such treatment for up to four weeks without noticeable changes in gel properties.

The experiment with the xanthan/LBG/agarose gel arranged inside the hyperthermia applicator demonstrated that the hydrogel can function as a water bolus during hyperthermia treatment. In contrast to the solution with water bags and other known water boli, the hydrogel does not require an added plastic layer. This results in an improved reflection coefficients, and hence the hydrogel water bolus exhibits excellent signal transmission from antennas. Moreover, the fact that the gel deformation is non-plastic, soft and non-brittle allows for close and better fit around different body shapes compared to the standard water bolus solutions. Nevertheless, we can foresee that use of the hydrogel water bolus in phased array arrangements requires a patient specific mould to guarantee an effective cooling and reproducible patient positioning. Having a mould available under the whole course of the treatment, provides an additional advantage of gel reparation if needed for instance due to evaporation or breakage of the gel.

5. Conclusions

This study shows that hydrogels has potential to be used as a water bolus during hyperthermia treatment. Compared with the commonly used water-filled plastic bags, the gel offers advantages, as it provides tight closure between the antenna and the gel, as well as between the gel and the body. The close fit between the different parts (antenna, gel, phantom), in combination with the permittivity of the gel being similar to that of water, results in reduced scattering of the waves, thus enabling more efficient heat delivery. In addition, the use of a gel enables an excellent agreement between predicted and experimentally measured interference.

Although the permittivity of all examined gels (HM pectin/alginate, xanthan/LBG, and xanthan/LBG/agarose) was similar to that of water, relatively high conductivity disqualified the use of the HM pectin/alginate gel. Further, only the ternary system of xanthan/LBG/agarose showed rheological and mechanical properties suitable for the intended use. Agarose gels, similarly to HM pectin/alginate gels, are strong and resistant to heat, but they are brittle. However, the combination of xanthan/LBG/agarose gives a soft and deformable three-component gel. This gel is characterized by the softness and deformability of xanthan/LBG at low temperatures and by the thermal hysteresis typical of agarose at higher temperatures.

While the hydrogel bolus still needs to be verified under clinical settings, we believe that the results presented here open up a new application area for hydrogels in improving hyperthermia treatment, and with potential in other microwave based near-field applications or ultrasound systems devoted to hyperthermia or thermal ablation. The acoustic properties of the suggested gels need to be determined prior to ultrasound applications. Further studies should focus on routes to improve the efficiency of cooling of the gel, control evaporation as well as determination of exact life-time of the gel.

Acknowledgment

Tuva Wegnelius, Stèphanie Hannoun, Björn Lönn and Liam Ekman, are acknowledged for their excellent experimental work. We also thank Christian Müller for interesting suggestion. This work was financially supported by the VINN Excellence Centre ChaseON (Chalmers Antenna Systems Centre) and SuMo Biomaterials, as well as Vinnova's VINNMER Marie Curie Chair.

ORCID iDs

Hana Dobšíček Trefná https://orcid.org/0000-0001-6025-0819
Anna Ström https://orcid.org/0000-0002-9743-1514

References

Arunachalam K, Maccarini P F, Schlorff J L, Birkelund Y, Jacobsen S and Stauffer P R 2009 Design of a water coupling bolus with improved flow distribution for multi-element superficial hyperthermia applicators *Int. J. Hyperth.* **25** 554–65
Cairns P, Miles M J and Morris V J 1986 Intermolecular binding of xanthan gum and carob gum *Nature* **322** 89–90
Cheetham N W, McCleary B V, Teng G, Lum F and Maryanto 1986 Gel-permeation studies on xanthan-galactomannan interactions *Carbohydrate Polym.* **6** 257–68
Cihoric N *et al* 2015 Hyperthermia-related clinical trials on cancer treatment within the clinicaltrials.gov registry *Int. J. Hyperth.* **31** 609–14
Copetti G, Grassi M, Lapasin R and Pricl S 1997 Synergistic gelation of xanthan gum with locust bean gum: a rheological investigation *Glycoconjugate J.* **14** 951–61
Datta N R, Puric E, Klingbiel D, Gomez S and Bodis S 2016 Hyperthermia and radiation therapy in locoregional recurrent breast cancers: a systematic review and meta-analysis *Int. J. Radiat. Oncol. Biol. Phys.* **94** 1073–87
Dewhirst M W, Vujaskovic Z, Jones E and Thrall D 2005 Re-setting the biologic rationale for thermal therapy *Int. J. Hyperth.* **21** 779–90
Draget K 2009 Alginates *Handbook of Hydrocolloids (Woodhead Publishing Series in Food Science, Technology and Nutrition)* 2nd edn, ed G O Phillips, P A Williams (Woodhead: Cambridge) ch 28, pp 807–28
Draget K and Taylor C 2011 Chemical, physical and biological properties of alginates and their biomedical implications *Food Hydrocolloids* **25** 251–6
Fatin-Rouge N, Milon A, Buffle J, Goulet R R and Tessier A 2003 Diffusion and partitioning of solutes in agarose hydrogels: the relative influence of electrostatic and specific interactions *J. Phys. Chem.* B **107** 12126–37
Fitzpatrick P, Meadows J, Ratcliffe I and Williams P A 2013 Control of the properties of xanthan/glucomannan mixed gels by varying xanthan fine structure *Carbohydrate Polym.* **92** 1018–25
Goycoolea F M, Richardson R K, Morris E R and Gidley M J 1995 Stoichiometry and conformation of xanthan in synergistic gelation with locust bean gum or konjac glucomannan: evidence for heterotypic binding *Macromolecules* **28** 8308–20
Hellerbach A, Schuster V, Jansen A and Sommer J 2013 MRI phantoms–are there alternatives to agar? *PLoS One* **8** 1–8
Hermansson E, Schuster E, Lindgren L, Altskär A and Ström A 2016 Impact of solvent quality on the network strength and structure of alginate gels *Carbohydrate Polym.* **144** 289–96
Higiro J, Herald T and Alavi S 2006 Rheological study of xanthan and locust bean gum interaction in dilute solution *Food Res. Int.* **39** 165–75
Kampinga H H 2006 Cell biological effects of hyperthermia alone or combined with radiation or drugs: a short introduction to newcomers in the field *Int. J. Hyperth.* **22** 191–6
Labille J, Thomas F, Milas M and Vanhaverbeke C 2005 Flocculation of colloidal clay by bacterial polysaccharides: effect of macromolecule charge and structure *J. Colloid Interface Sci.* **284** 149–56
Lee K Y and Mooney D J 2012 Alginate: properties and biomedical applications *Prog. Polym. Sci.* **37** 106–26
Lundin L and Hermansson A M 1995 Supermolecular aspects of xanthan-locust bean gum gels based on rheology and electron microscopy *Carbohydrate Polym.* **26** 129–40
Mannion R O, Melia C D, Launay B, Cuvelier G, Hill S E, Harding S E and Mitchell J R 1992 Xanthan/locust bean gum interactions at room temperature *Carbohydrate Polym.* **19** 91–7
Morris V J and Chilvers G R 1984 Cold setting alginate-pectin mixed gels *J. Sci. Food Agric.* **35** 1370–6
Normand V, Aymard P, Lootens D L, Amici E, Plucknett K P and Frith W J 2003 Effect of sucrose on agarose gels mechanical behaviour *Carbohydrate Polym.* **54** 83–95
Norton I T, Goodall D M, Austen K R J, Morris E R and Rees D A 1986 Dynamics of molecular organization in agarose sulphate *Biopolymers* **25** 1009–29
Overgaard J 2013 The heat is (still) on-the past and future of hyperthermic radiation oncology *Radiother. Oncol.* **109** 185–7
Renou F, Petibon O, Malhiac C and Grisel M 2013 Effect of xanthan structure on its interaction with locust bean gum: toward prediction of rheological properties *Food Hydrocolloids* **32** 331–40
Rijnen Z, Togni P, Roskam R, van de Geer S G, Goossens R H and Paulides M M 2015 Quality and comfort in head and neck hyperthermia: a redesign according to clinical experience and simulation studies *Int. J. Hyperth.* **31** 823–30
Serwer P 1983 Agarose gels: properties and use for electrophoresis *Electrophoresis* **4** 375–82
Strange D G T, Fletcher T L, Tonsomboon K, Brawn H, Zhao X and Oyen M L 2013 Separating poroviscoelastic deformation mechanisms in hydrogels *Appl. Phys. Lett.* **102** 031913–7
Ström A and Williams M A 2004 On the separation, detection and quantification of pectin derived oligosaccharides by capillary electrophoresis *Carbohydrate Res.* **10** 1711–6
Ström A, Boers H, Koppert R, Melnikov S, Wiseman S and Peters H 2009 Physico-chemical properties of hydrocolloids determine their appetite effects *Gums Stabilisers Food Ind.* **15** 341
Sworn G 2009 Xanthan gum *Handbook of Hydrocolloids* (*Woodhead Publishing Series in Food Science, Technology and Nutrition*) 2nd edn, ed G O Phillips and P A Williams (Cambridge: Woodhead) ch 8, pp 186–203
Takook P, Persson M, Gellermann J and Trefna H D 2017 Compact self-grounded bow-tie antenna design for an UWB phased-array hyperthermia applicator *Int. J. Hyperth.* **33** 387–400

Trefna H D *et al* 2017a Quality assurance guidelines for superficial hyperthermia clinical trials: I. Clinical requirements *Int. J. Hyperth.* **33** 471–82

Trefna H D *et al* 2017b Quality assurance guidelines for superficial hyperthermia clinical trials: II. Technical requirements for heating devices *Strahlenther Onkol.* **193** 351–66

Trefna H D, Shafiemehr M and Persson M 2016 Laboratory prototype of UWB applicator for head and neck hyperthermia *12th Int. Congress on Hyperthermic Oncology* pp e425–31

Trefna H D, Togni P, Shiee R, Vrba J and Persson M 2012 Design of a wideband multi-channel system for time reversal hyperthermia *Int. J. Hyperth.* **28** 175–83

Walkenström P, Kidman S, Hermansson A M, Rasmussen P B and Hoegh L 2003 Microstructure and rheological behaviour of alginate/pectin mixed gels *Food Hydrocolloids* **17** 593–603

Watase M and Nishinari K 1983 Rheological properties of agarose gels with different molecular weights *Rheol. Acta* **22** 580–7

Wielinga W 2009 Galactomannans *Handbook of Hydrocolloids* (*Woodhead Publishing Series in Food Science, Technology and Nutrition*) 2nd edn, ed G O Phillips and P A Williams (Cambridge: Woodhead) ch 10, pp 228–51

Zhan D, Ridout M, Brownsey G and Morris V 1993 Xanthan-locust bean gum interactions and gelation *Carbohydrate Polym.* **21** 53–8

Zhao X, Huebsch N, Mooney D J and Suo Z 2010 Stress–relaxation behavior in gels with ionic and covalent crosslinks *J. Appl. Phys.* **107** 063509